Proton Energy Loss Spectroscopy for Surface Monolayer Analysis

Noriaki Matsunami
Nagoya University

Utah State University
MERRILL-CAZIER LIBRARY

PROTON ENERGY LOSS SPECTROSCOPY FOR SURFACE MONOLAYER ANALYSIS

Noriaki Matsunami

Crystalline Materials Science, Faculty of Engineering
Nagoya University
Furo-cho, Chikusa-ku, Nagoya 464, Japan
Phone no : 052-781-5111

Abstract

A survey is given of recent advances in the use of high-energy proton back-scattering spectroscopy or proton energy loss spectroscopy (PELS) under the glancing incidence geometry for mono-layer-sensitive analysis. Two theories of the energy loss involved in the PELS are described, based on the continuous and impact parameter dependent slowing down models. The latter theory leads to the azimuthal angle dependence of the energy loss. It is also shown that this technique is applicable to underlayer composition analysis.

Introduction

A well-defined ion beam with the energy of 0.1 - 1 MeV per nucleon, typically collimated to less than 0.1 degree and 0.1 cm, has been employed extensively for analyzing the atomic structure of solid surfaces and the composition near solid surfaces (Feldman, 1981; Feldman and Mayer, 1986; Van der Veen, 1985; Chu et al., 1978). At these energies, the elastic scattering or change in the direction of ions by atoms is fully described by the classical trajectory picture, i.e., no diffraction comes into play. The term elastic scattering is used to designate the scattering which excludes ionization and excitation of electrons. Furthermore, the high energy ion-atom interaction is characterized by low neutralization (Buck et al., 1973; Buck, 1977; Ross and Terreaut, 1986), well-defined elastic scattering cross section and small angular deviation between two successive elastic scatterings. During the scattering, the ion loses energy elastically by an amount dependent on the target atomic mass as well as inelastically by colliding with electrons. Two assumptions were made, namely, that the inelastic energy loss is proportional to the ion path length and the single scattering is dominant and both are valid under usual conditions of near surface analysis. This constitutes the basis of the depth and composition analysis in the high energy ion scattering spectroscopy. Hence, the layer-by-layer composition analysis is plausible, if the resolution is good enough. The composition of each surface layer would be fundamental to understanding surface structures.

The energy resolution of surface barrier solid state detectors which are most frequently used in the high energy ion scattering experiments is about 10 keV, corresponding to the depth resolution of 10 nm. The glancing scattering geometry improves the depth resolution to approximately 3 nm

(Williams, 1978). For single crystal samples, the depth resolution can be increased effectively by using the channeling and/or blocking effect (Bogh 1973; Davies et al., 1975). The other types of energy analyzers such as electrostatic analyzer (Wijngaarden et al., 1971; Turkenburg et al., 1976; Smeenk et al., 1982; Graham et al., 1986), magnetic analyzer (Hirvonen and Hubler, 1976; Bogh, 1973) and time of flight (Chevarier et al., 1981; Chevarier and Chevarier, 1983) give better resolution of several hundred eV or 1 nm. These, however, are not sufficient for layer-by-layer analysis.

In order to improve the resolution, the present authors have developed the high-resolution proton energy loss spectroscopy and obtained the best resolution of 20 eV for 100 keV protons (Matsunami et al., 1983; Oku et al., 1986). The high resolution is achieved utilizing the method developed by Park and Schowengerdt (1969) for ion-gas target collision studies, where the energies of scattered protons are analyzed after decelerating to 1 keV. At present, the glancing incidence geometry, the scattering angle being 12 degrees, is adopted to have reasonable counting rate and to minimize the surface roughness effects.

This paper describes the high-resolution proton energy loss spectroscopy (PELS) at glancing incidence geometry. The experimental system is described in next section. Theories of the energy loss involved in the PELS, based on the continuous and impact parameter dependent slowing down models are discussed after the experimental section. It is shown that the energy loss calculated with the latter model depends on the azimuthal angle or rotation angle around the surface normal. Next, the measured energy loss spectra of 100 keV protons for a gold film on a Si(111) surface are shown. The applicability of PELS to layer-by-layer analysis is discussed.

Experimental

A schematic of high-resolution proton energy loss spectrometer with the glancing incidence geometry, which has been developed at Nagoya (Matsunami et al., 1983; Oku et al., 1986), is shown in Fig. 1. The method of attaining high resolution is similar to that developed by Park and Schowengerdt (1969). Protons are generated with a hollow cathode ion source (Danfysik 911A) and are accelerated to the acceleration voltage V_a ~100 kV, the stability of V_a being ~20 V at V_a = 100 kV. The protons are deflected by 62 degrees with a magnet and introduced into an Ultra-High-Vacuum scattering chamber.
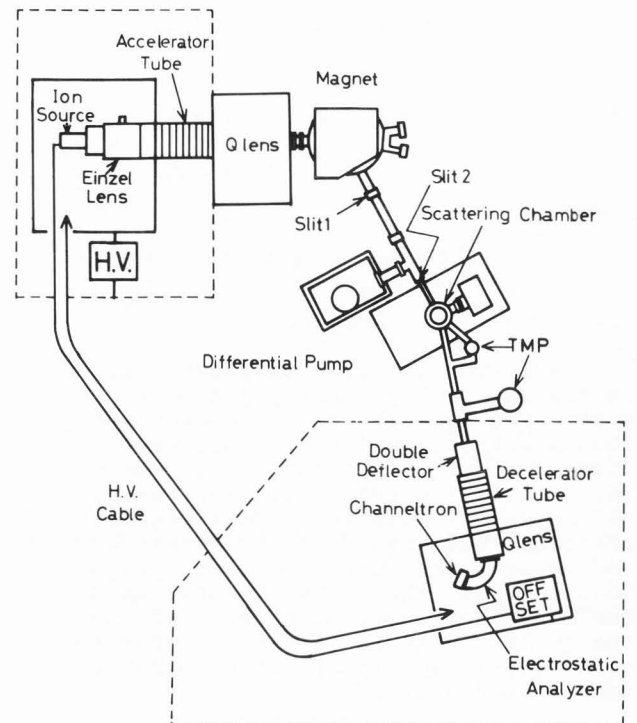

Fig. 1. A sketch of the high-resolution proton energy-loss spectrometer (after Oku et al., 1986).

The incident proton beam is collimated to 0.022 and 0.064 degrees in the horizontal and vertical directions, respectively.

Scattered protons from a solid surface are decelerated to an offset voltage V_O of a few kV. The same power supply is used for both the acceleration and the deceleration stages, i.e., the deceleration voltae V_d is equal to $V_a - V_O$. The energy resolution is greatly increased by performing the energy analysis at reduced energies. Referring to Fig. 2, the energy loss ΔE of the scattered protons is given by:

$$\Delta E = q(V_a - V_d) - E_f = qV_O - E_f . \quad (1)$$

Here q is the charge of a proton and E_f is the energy of protons which can pass through the electrostatic analyzer and are detected with a channeltron (or a Faraday cup for measurement of resolution). Since Eq. (1) does not include the acceleration voltage, ripples of V_a are cancelled out. However, the cancellation is incomplete particularly for the high frequency component of V_a, because of the flight time of protons, which is ~1 µs in this case. The incomplete ripple cancellation is a factor
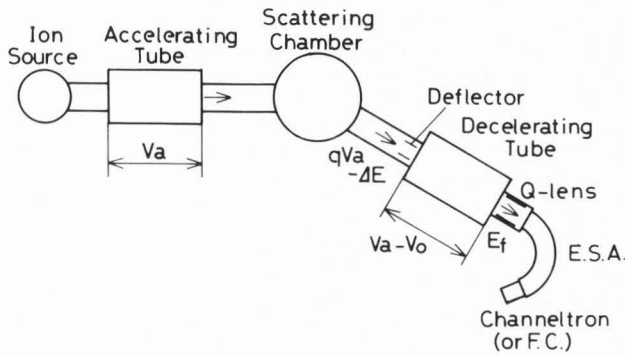
Fig. 2. Diagram of the variation of the ion beam energy in the high-resolution proton energy loss spectroscopy technique.

determining the resolution.

The energy loss spectrum is obtained by varying the offset voltage V_O, E_f being fixed (usually 1 keV). In order to increase the counting efficiency, a metallic mesh which reduces the divergence of the electric field beyond the end of the deceleration tube is incorporated at the final stage of the deceleration tube and a quadrapole lens is inserted between the deceleration tube and the electrostatic analyzer.

The energy resolution of the present apparatus is measured under the condition of no scattering or $\Delta E=0$, as a function of the size $\tilde{W}$ of the entrance and exit slits of the electrostatic analyzer (Oku et al., 1986). Both slits have the same size. The results are shown in Fig. 3a for 100 keV H^+. The efficiency is normalized to the current just before entering the electrostatic analyzer. The resolution in FWHM (full width at half maximum) is plotted in Fig. 3b as a function of the slit size. The resolution is found to be proportional to $\tilde{W}$. The best resolution is 18 eV. The energy spread in the ion source and the incomplete cancellation of ripples of the acceleration-deceleration voltage would explain the resolution. The deviation from the linear dependence of FWHM on $\tilde{W}$ at $\tilde{W}=2.0$ is partly due to the fact that the resolution is sensitive to the alignment of the energy analyzer system. Further investigation, such as measurement of the resolution as a function of V_a and E_f, should be done to improve the resolution.

Theory of Energy Loss

Models

Energy loss is a fundamental quantity involved in the use of the PELS technique. Computer simulation is required to obtain accurate intensity distributions of the energy loss. The computer simulation,
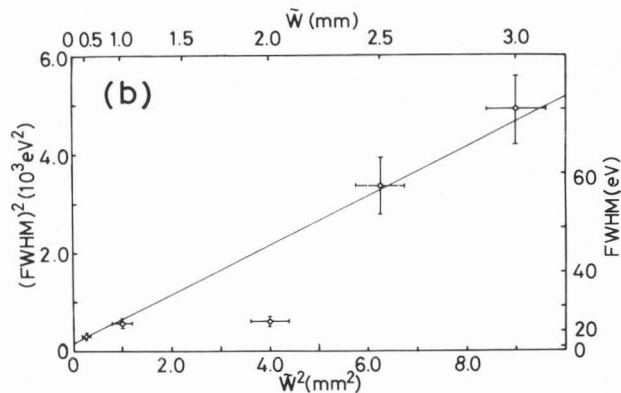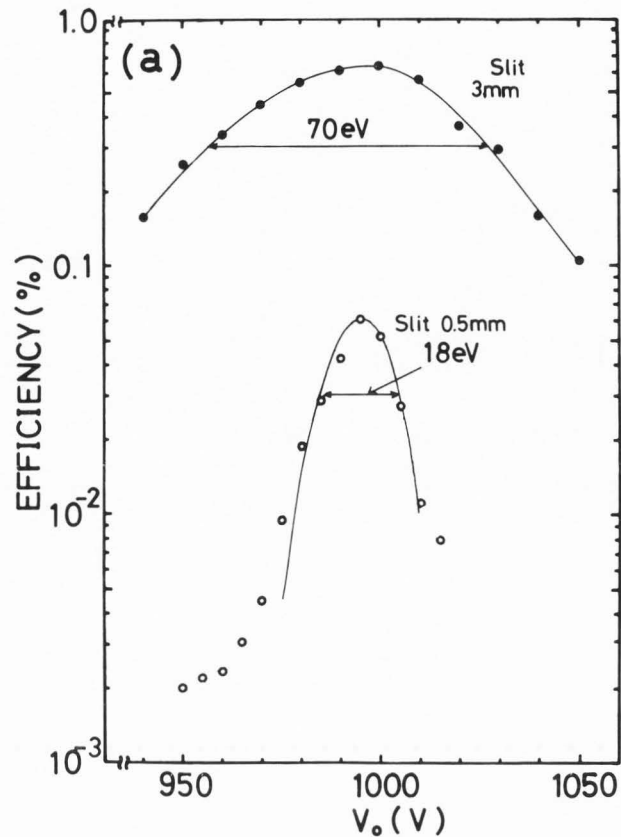

Fig. 3. (a) Energy spectra of 100 keV protons after decelerating to 1 keV, under no scattering condition, measured with ESA slit widths of 0.5 mm (open circles) and of 3 mm (closed circles). (b) Relation between the energy resolution (FWHM) and the slit width $\tilde{W}$, (after Oku et al., 1986).

however, is found to be very time consuming. Thus simple, analytical and less time-consuming theories are desired. Two analytical models are discussed in this section, which can be used to calculate the energy loss of

scattered protons, disregarding their intensity. Both models assume that the single elastic scattering is dominant, as mentioned in "Introduction". In addition, the first model assumes that the inelastic energy loss is proportional to the ion path length. This model, which involves single scattering and continuous slowing down (SSCSD), is applicable basically to a non-crystalline solid. This model is the one most frequently used in high-energy ion scattering spectroscopy.

The second model assumes that the inelastic energy loss per atom depends on the impact parameter, instead of the path length. The model, single scattering and impact parameter dependent slowing down (SSIPSD), may be applicable to crystalline solids under glancing incidence geometry. It appears that the energy loss calculated with the model depends on the azimuthal angle, which is the rotation angle around the axis normal to the surface.

Single scattering and continuous slowing down

The details of the single scattering and continuous slowing down model are described elsewhere (Chu et al., 1978; Feldman and Mayer, 1986). The basic point is reproduced here. As shown in Fig. 4, suppose that a well-defined parallel ion beam with an energy E_O is incident on a solid surface and scattered from the surface. The angles between the incoming and outgoing ion beam directions and the surface are θ_1 and θ_2, respectively. The scattering angle is equal to $\theta_1+\theta_2$. The surface is assumed to be ideal and static. Making use of the assumptions mentioned before, the inelastic energy loss values along the incoming and outgoing paths are written, $S_1X/\sin\theta_1$ and $S_2X/\sin\theta_2$, respectively. Here X is the depth including the effective depth $X_e=\bar{d}\cdot\lambda$ from the surface to the top atomic plane:

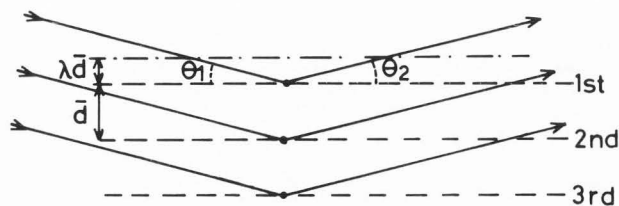$$X=j*\bar{d}+X_e=(j+\lambda)*\bar{d}, \quad j=0,1,2\ldots \quad (2)$$

The effective depth takes care of the extension of the electron wavefunction outside the top atomic plane. This is neglected in the usual high-energy ion scattering spectroscopy. S_1 and S_2 are the stopping powers appropriate for the incoming and outgoing paths, respectively. These are well approximated as the stopping powers at E_O and KE_O, where K is the kinematic factor for scattering angle θ. Disregarding energy straggling, the total energy loss ΔE is given by (Oku et al., 1986),

$$\Delta E=(1-K)E_o+(KS_1/\sin\theta_1+S_2/\sin\theta_2)X . \quad (3)$$

The first term and the second term represent the elastic and inelastic energy losses, respectively.

For near surface analysis and glancing scattering geometry ($K\approx1$), S_2 can be replaced by S_1, thus Eq. (3) reads as:

$$\Delta E=(1-K)E_o+S_1X(K/\sin\theta_1+1/\sin\theta_2) . \quad (4)$$

In table 1, the values of S_1, $\bar{d}$ and ΔE are listed for 100 keV protons in Si, W and Au at $\theta_1=\theta_2=6°$. Here $X=\bar{d}/2$, $\bar{d}=N^{-1/3}$ (j=0 and $\lambda=1/2$), N being the atomic density, are used to evaluate ΔE. Also employed are the tabulated values of stopping powers (Andersen and Ziegler, 1977). In this case, X is equal to a half of the average layer-separation $\bar{d}$. Also listed is the energy straggling Ω (Besenbacheur et al., 1980, 1981; Kaneko and Yamamura, 1986). The energy straggling is defined as the second moment of the energy loss distribution due to stat-

Table 1. Stopping power S_1, average layer-separation $\bar{d}$, energy loss ΔE calculated with the SSCSD model and energy straggling Ω for 100 keV H^+ at incoming and outgoing angles of 6° (see text). Here $\lambda=1/2$ is used.

	S_1 $\dfrac{eV}{nm}$	$\bar{d}$ (nm)	ΔE (eV)			Ω (eV)
			Total	Elastic	Inelastic	
Si	120	0.272	469	157	312	138
W	224	0.251	562	24	538	216
Au	225	0.259	579	22	557	212

Fig. 4. Schematic ion trajectories in ion-surface scattering. Dashed lines indicate atomic planes.

istical nature in the energy loss process. Precisely speaking, the term energy loss means the first moment of the energy loss distribution, i.e., the average energy loss. It should be noted that the energy straggling is smaller than the energy loss. This makes the layer-by-layer analysis simple.

Kawai et al. (1982) have done a computer simulation of the energy loss for 100 keV protons on a Ni(100) surface at $\theta_1=\theta_2=0.5°$. The result is shown in Fig. 5. They obtained the energy loss peak at 1.65 keV and the energy straggling of 83 eV. In their calculation, $X=\overline{d}/2=0.088$ nm is used. The continuous slowing down model gives an inelastic energy loss of 3.1 keV and energy straggling of 415 eV. These values are larger than those of the computer simulation. This result reveals the importance of the impact parameter dependent inelastic energy loss for ion-surface scattering.
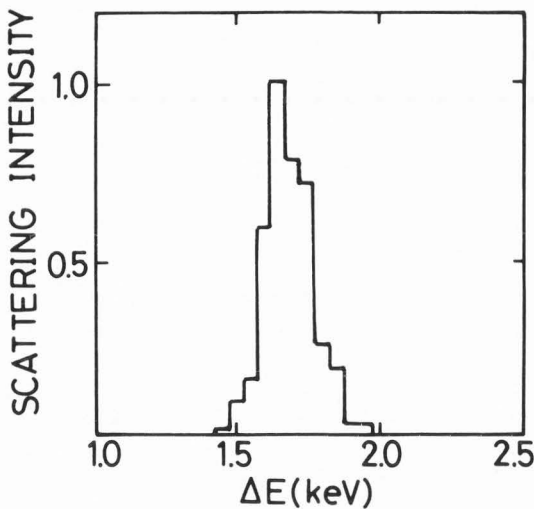

(a)

axis normal to surface

crystal

(b)

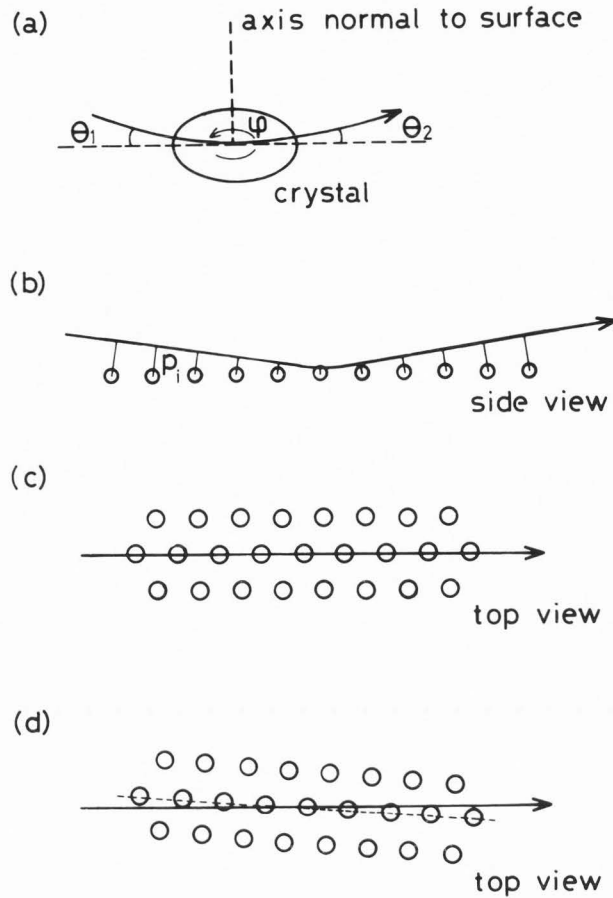side view

(c)

top view

(d)

top view

Fig. 6. (a) Schematic ion trajectories, (b) Side view of ion trajectories, illustrating an impact parameter p_i, (c) Top view of ion trajectories, (d) The same as (c), except that a crystal is rotated around the axis normal to the surface.

Fig. 5. Energy loss spectrum of 100 keV proton on Ni(100) surface for $\theta_1=\theta_2=0.5°$, azimuthal angle ψ of 20° from a <100> axis, acceptance angle of $\Delta\theta=\Delta\psi=0.15°$ (after Kawai et al., 1982).

Single scattering and impact parameter dependent slowing down

The model of the single scattering and impact parameter dependent slowing down (SSIPSD) is also based on the linear trajectories of ions incident on a crystalline solid surface as shown in Fig. 6. Using the fact that an ion collides with an atom at the impact parameter for a given trajectory, the inelastic energy loss is written as:

$$\sum_i S(p_i) \quad . \qquad (5)$$

Here S(p) is the inelastic energy loss per atom for an impact parameter p. For a crystalline solid surface, it can be easily seen that the impact parameter distribution depends on the azimuthal angle, i.e., rotation angle around the axis normal to the surface, as shown in Fig. 7. The inelastic energy loss is calculated as a function of the azimuthal angle for 100 keV protons on a W(111) surface at $\theta_1=\theta_2=6°$. In the present calculation, the analytical form derived by Oen and Robinson (1976) is used:

$$S(p) = \alpha \exp(-0.3p/a) \quad . \qquad (6)$$

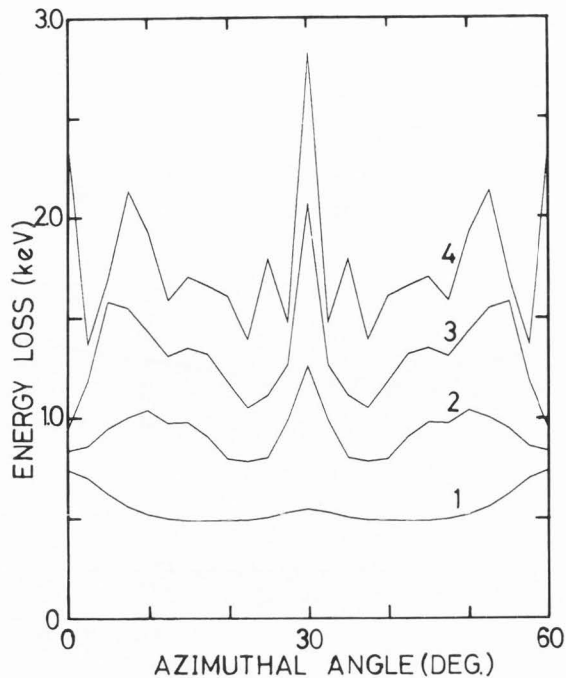Here a is the Thomas-Fermi screening radius and $\alpha=0.045S_1/a\ N^2$ is the normalization factor such that

Fig. 7. Calculated inelastic energy loss as a function of the azimuthal angle ψ measured from a <110> axis for 100 keV H^+ on W(111) at $\theta_1 = \theta_2 = 6°$. The numbers in the figure mean the layer at which protons are scattered elastically. The Oen and Robinson (1976) model is used for the impact parameter dependent energy loss.

$\int 2\pi p S(p) dp = S_1$, S_1 being given in Table 1. The azimuthal angle is measured from a <110> axis of a W(111) surface. Again, the scattering intensity and energy straggling are neglected. The energy loss at the 1st, 2nd, 3rd and 4th layers is indicated by the corresponding number in the figure. The azimuthal angle dependence of the energy loss would be a test of continuous and impact parameter dependent slowing down model.

Application to Surface Analysis

The PELS technique is demonstrated by analyzing a clean and Au covered Si(111) surfaces. The results are shown in Fig. 8 (Oku et al., 1986). The scattering angle was 12° and the resolution was 180 eV in order to have reasonable scattering intensity. The gold coverage before annealing was estimated to be 1.4 monolayer. The proton beam current was about 20 nA, The base pressure was 6×10^{-8} Pa and the pressure during measurement was 3×10^{-7} Pa. Proton beams of 5 μC and 2.5 μC for each point were used for Si and Au/Si surface, respectively. The beam size was approximately 0.4×1 mm^2.
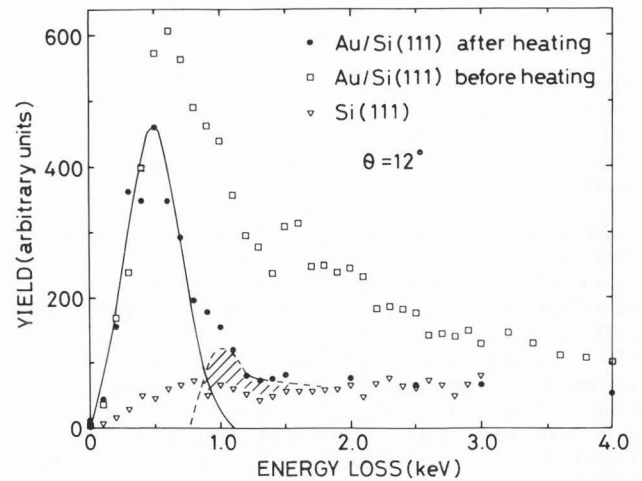Three possible beam effects are

Fig. 8. Energy loss spectra of 100 keV protons at a scattering angle of 12° for a clean Si(111) surface (triangles) and an Au-deposited Si(111) surface before (squares) and after (closed circles) annealing at 900°C for 15 s. The solid line is a Gaussian fit to the low energy loss region of the peak.

discussed. Since the incident angle was 6°, the beam size on the sample was approximately 4×1 mm^2. Hence the proton fluence was~4×10^{14}/cm^2 for 2.5 μC and total fluence was~2×10^{16}/cm^2. Firstly, the proton energy is high so that the protons are implanted deep in the sample, the projected range of 100 keV H^+ in Si being 1 μm (Andersen and Ziegler, 1977). Moreover, in terms of the implantation, the fluence is relatively small. Thus the implantation effect on this analysis is not significant. Secondary, dpa (displacement per atom) for Au was estimated to be 0.7×10^{-3} for 4×10^{14}/cm^2, assuming that the displacement energy is 25 eV. For Si, dpa is smaller by a factor of 3. Therefore, damage induced by incident protons is not important. Finally, the sputtering yield Y was estimated to be 1.4×10^{-3} (n=1) and 0.014 (n=2) for Si, and 0.022 (n=1) and 0.22 (n=2) for Au at the proton energy of 100 keV and the angle $\theta_1 = 6°$, using the relation Y=Y(normal incidence)/$(\sin\theta_1)^n$ with n=1~2 (Matsunami et al., 1984; Yamamura, 1984). The fluence of 4×10^{14}/cm^2 is comparable with the surface atom density. Thus the proton induced sputtering may reduce the PELS yield by 1 ~ several 10 %, depending on the n value. In fact, for Au covered Si(111) surface, 20 % reduction in the yield was observed at a fluence of ~1.6×10^{16}/cm^2. This could be due to proton induced sputtering.

In Fig. 8, a broad peak for clean Si(111) is seen at the energy loss of ~800 eV (open circles). This energy

loss agrees with the value in Table 1 within a factor of two, indicating that the broad peak originates from the top or the first double layer of Si(111) surface. Further analysis needs a computer simulation and the appropriate impact parameter dependent inelastic energy loss function.

For a gold covered Si(111) surface before annealing, the energy loss spectrum exhibits a peak at 600 eV and a tail extending to 4 keV (open squares). After annealing at 900°C for 15 s, the peak of the energy loss spectrum shifts to 500 eV and the yield extending to 4 keV reduces to that of pure Si, except the shoulder at ~1 keV. The gold coverage after annealing was estimated to be about 0.5 monolayer. This value was in good agreement with that measured at a different chamber by means of Rutherford Backscattering Spectroscopy of 1.5 MeV He. The spectrum is fitted by a Gaussian as indicated by the solid line with the full-width at half maximum(FWHM) of 500 eV. Here, FWHM is equal to 2.35 times the energy straggling Ω. This value yields 470 eV after correcting the experimental resolution of 180 eV. Suppose an atomic plane that consists of one monolayer of Si and 0.5 monolayer of Au, the energy loss and straggling are estimated with the SSCSD model to be 430 eV and 469 eV, respectively. The experimental values are in good agreement with the calculated values, indicating that the Gaussian part represents the top layer gold atoms. However, it should be noted again that the computer simulation with an appropriate inelastic energy loss function is required for the detail analysis.

By subtracting the Gaussian intensity from the experimental intensity, the dashed line is obtained with a peak at ~1 keV. Since the larger energy loss means that gold atoms are located below the top layer, the shaded part enclosed by the dashed line and Si intensity line represents the gold atoms located at under layer. The fraction of gold atoms located at under layer is approximately 10 % of all gold atoms.

The present observations that a stable Au layer is formed on a Si(111) surface upon high temperature annealing are consistent with observations by photoemission spectroscopy (Cao et al., 1986; Braicovich et al., 1979) and by electron energy loss spectroscopy (Salvan et al., 1980) that a single ordered monolayer of Au is present at the surface upon annealing of 1-20 ML of Au above 650°C. However this does not mean inconsistency with observations by spatially resolved Auger electron spectroscopy (Perfetti et al., 1982; Calliari et al., 1984) that a very small fraction of Au is converted into clusters or islands upon annealing. Because islands or clusters of a very small fraction of Au cause broadening of the energy loss peak by a small amount.

Concluding Remarks

High-resolution proton energy loss spectroscopy (PELS) is described for monolayer-sensitive analysis. The best resolution is obtained to be 18 eV for 100 keV protons. Two analytical theories are given to calculate the inelastic energy loss. The theory based on the impact parameter dependent slowing down leads to an azimuthal angle dependence of the inelastic energy loss for crystalline solid surfaces.

For Au deposited Si(111) surface, the energy loss spectrum shows a peak with a tail or shoulder. It is found that the Gaussian part of the spectrum is ascribed to scattering from gold atoms at the top layer of the Au/Si(111) surface. It is suggested that the shoulder part of the energy loss spectrum is due to scattering from gold atoms below the top layer.

In summary, the present PELS at glancing scattering geometry can be applicable to surface layer-by-layer analysis with sensitivity of a few tenths of monolayer. This is useful for adsorbate with high atomic number on substrate consisting of low atomic numbers or for light adsorbate on heavy substrate, because of poor mass resolution of PELS at glancing scattering geometry.

Acknowledgements

References

Andersen H H, Ziegler J F (1977) Hydrogen Stopping Powers And Ranges In All Elements. Pergamon Press, New York, 1-317.

Besenbacheur F, Andersen J U, Bonderup E (1980) Straggling In Energy Loss of Energetic Hydrogen and Helium Ions. Nucl. Instrum. & Meth. 168, 1-15.

Besenbacheur F, Andersen H H, Hvelplund P, Knudsen H (1981) Straggling In Energy Loss of Swift Hydrogen and Helium Ions in Gases. Mat. Fys. Medd. Dan. Vid. Selsk, 40 no 9 1-42.

Bogh E (1973) Application To Surface Studies. In: Channeling. Morgan D V (ed), Wiley, London, 435-451.

Braicovich L, Garner C M, Skeath P R, Su C Y, Chye P W, Lindau I, Spicer W E (1979) Photoemission studies of the Silicon-Gold Interface. Phys. Rev. B20, 5131-5141.

Buck T M, Wheatley G H, Feldman L C (1973) Charge States of 25-150 keV H And ^{4}He Backscattered From Solid Surfaces. Surf. Sci. 35, 345-361.

Buck T M (1977) Neutralization Behavior in Medium Energy Ion Scattering In: Inelastic Ion-Surface Collisions, Tolk N H, Tully J C, Heiland W , White C W (eds), Academic Press, New York, 47-71.

Calliari L, Sancrotti M, Braicovich L (1984) Agglomeration at Si/Au interfaces: A Study with Spatially Resolved Auger Line-Shape Spectroscopy. Phys. Rev. B30, 4885-4887.

Cao R, Yeh J J, Nogami J, Lindau I (1986) Summary Abstract: Photoemission Study of the Annealed Au/Si Interface. J. Vac. Sci. Technol. A4, 846-847.

Chevarier A, Chevarier N, Chiodelli S (1981) A high Resolution Spectrometer Used In MeV Heavy Ion Backscattering Analysis. Nucl. Instrum. & Meth. 189, 525-531.

Chevarier A, Chevarier N (1983) Time of Flight Spectrometry In Heavy Ion Backscattering Analysis. Nucl. Instrum. & Meth. 218, 1-5.

Chu W K, Mayer J W, Nicolet M A (1978) Backscattering Spectrometry. Academic Press, New York, 1-384.

Davies J A, Jackson D P, Mitchell J B, Norton P R, Tapping R L (1975) Measurement of Surface Relaxation By MeV Ion Backscattering And Channeling. Phys. Lett. 54A, 239-240.

Feldman L C (1981) Atomic Position of Surface Atoms Using High Energy Ion Scattering. Nucl. Instrum. & Meth. 191, 211-219.

Feldman L C, Mayer J W (1986) Fundamentals Of Surface And Thin Film Analysis. North-Holland, New York, 1-352.

Graham W R, Yalisone S M, Adams E D, Gustabsson T, Copel M, Tornqvist E (1986) Comparison of Solid State And Electrostatic Particle Detection In Medium Energy Ion Scattering With Channeling And Blocking. Nucl. Instrum & Meth. B16, 383-390.

Hirvonen K J, Hubler G K (1976) Application of A High Resolution Magnetic Spectrometer To Near-Surface Materials Analysis. In: Ion Beam Surface Layer Analysis, Mayer O, Linker G, Kappeler F (eds), Plenum Press, New York, 457-469.

Kaneko T, Yamamura Y (1986) Energy Straggling of Light-Ion Beam. Phys. Rev. A33, 1653-1660.

Kawai R, Itoh N, Ohtsuki Y H (1982) Inelastic Scattering Of Ions At The Surface. Surf. Sci. 114, 137-146.

Matsunami N, Oku T, Horino Y, Ozaki H, Itoh N, Matsuda K (1983) High-Resolution Proton-Energy-Loss Spectroscopy For Surface Analysis. In: Proc. Int. Ion Engineering Congress-ISIAT '83 & IPAT '83, Takagi T (ed), (Kyoto 1983), 1907-1911.

Matsunami N, Yamamura Y, Itikawa Y, Itoh N, Kazumata Y, Miyagawa S, Morita K, Shimizu R, Tawara H (1984) Energy Dependence Of The Ion Induced Sputtering. Atomic Data and Nucl. Data Tables 31, 1-80.

Oen O S, Robinson M T (1976) Computer Studies Of The Reflection Of Light Ions From Solids. Nucl. Instrum. & Meth. 132, 647-653.

Oku T, Kanasaki J. Matsunami N, Itoh N, Matsuda K, Aoki M (1986) Proton Energy Loss Spectroscopy For Surface Layer Analysis In The Monolayer Regime. Nucl. Instrum. & Meth. B15, 142-145.

Park J T, Schowengerdt F D (1969) A Heavy-Ion Energy Loss Spectrometer. Rev. Sci. Instrum. 40, 753-760.

Perfetti P, Nannarone S, Patella F, Quaresima C, Capozi M, Savoia A, Ottaviani G (1982) Low-Energy Electron-Loss Spectroscopy and Auger-Electron-Spectroscopy Studies of Noble-Metal-Silicon Interfaces: Si-Au System. Phys. Rev. B 26, 1125-1138.

Ross G G, Terreaut B (1986) H^{-}, $H°$, H^{+}, $He°$, He^{+} and He^{2+} Fractions of Projectiles Scattered From 14 Different Materials At 30 To 340 keV. Nucl. Instrum. & Meth. B15, 146-150.

Salvan F, Cros A, Derrien J (1980)
Electron Energy Loss Measurements on the
Gold-Silicon Interface. J. Physique Lett.
41, L337-340.

Smeenk R G, Tromp R M, Kersten H H,
Boerboom A J H, Saris F W (1982) Angle
Resolved Detection Of Charged Particles
With A Novel Type Toroidal Electrostatic
Analyser. Nucl. Instrum. & Meth. 195,
581-586.

Turkenburg W C, Soszka W, Saris F W,
Kersten H H, Colenbraudev B G (1976)
Surface Structure Analysis By Means Of
Rutherford Scattering: Methods To Study
Surface Relaxation. Nucl. Instrum. & Meth.
132, 587-602.

Van der Veen J F. (1985). Ion Beam
Crystallography Of Surfaces And
Interfaces. Surf. Sci. Rept. 5, 199-288.

Wijngaarden A Van, Miremadi B,
Baylis W E. (1971). Energy Spectra Of keV
Backscattered Protons As A Probe For
Surface Regions. Can. J. Phys. 49,
2440-2448.

Williams J S (1978) The Application Of
High-Resolution Rutherford Backscattering
Techniques To Near-Surface Analysis. Nucl.
Instrum. & Methods 149, 207-217.

Yamamura Y (1984) An Empirical Formula
For Angular Dependence Of Sputtering
Yields. Radiation Effects 80, 57-72.

Discussion with Reviewers

L. B. Church: Compared to a standard XPS
or Auger spectrometer, what is the
relative cost of a PELS instrument?
Author: I would think that the cost of
UHV chamber is ~0.1 million $ and that of
accelerator and analyzer for PELS is ~0.4
million $. The total cost of PELS will be
comparable with that of ESCA.

C. Boiziau: It seems that the knowledge
of the main components of the solid
surface is necessary for the calculations
to be performed. Moreover, the
calculations seem necessary to interpret
accurately the experimental results. Is
thus the term "analysis" the good one for
such a technique?
Author: For analysis, the calculation is
very important as you pointed out. We
have to understand the energy loss process
in this PELS technique for detail
"analysis". To do this, we need precise
knowledge of the impact parameter
dependent energy loss. At present, no
good theory exists. Therefore we do two
types of experiments : one is for
obtaining the impact parameter dependent
energy loss (under progress now) and the

other is for demonstration of
applicability of this technique to
surface analysis. I suspect that the
problem is solved at the same time.

P. Kruit: Microscopists always want to
know the spatial resolution of a
technique. How small can you focus the
proton probe and yet have enough signal
for a reasonable analysis?
Author: We can focus proton beam to
µm. However, because of damage and
sputtering effects, the spatial
resolution would be limited to mm or sub
mm.